IEEE Access
Multidisciplinary | Rapid Review | Open Access Journal

SPECIAL SECTION ON EMERGING TECHNOLOGIES FOR ENERGY INTERNET

Received July 22, 2019, accepted August 19, 2019, date of publication August 22, 2019, date of current version September 9, 2019.

Digital Object Identifier 10.1109/ACCESS.2019.2936889

Incentive-Compatible Market Clearing for a Two-Stage Integrated Electricity-Gas-Heat Market

MANYUN HUANG, (Student Member, IEEE), ZHINONG WEI, (Member, IEEE), PING JU, (Senior Member, IEEE), JINRAN WANG, AND SHENG CHEN, (Student Member, IEEE)

College of Energy and Electrical Engineering, Hohai University, Nanjing 210098, China

Corresponding author: Zhinong Wei (wzn_nj@263.net)

This work was supported in part by the National Natural Science Foundation of China under Grant 51877071, in part by the Natural Science Foundation of Jiangsu Province, China, under Grant BK20171433, and in part by the Science and Technology Project of State Grid Jiangsu Electric Power Corporation (Research on key technologies and applications of precise customization of user-side integrated energy based on data drive under Grant J2019017).

ABSTRACT The establishment and development of an integrated energy market (IEM) contributes to the equitable distribution of electrical and thermal energy production resources. However, the application of conventional locational marginal price theory generally fails to promote the declaration of truthful marginal costs by market participants in the process of clearing and settlement of the IEM, which detracts from market fairness and may reduce market efficiency. Simultaneously, the continuous expansion in the scale of renewable energy sources (RESs) threatens the safe and stable operation of electrical power systems. Accordingly, the present study seeks to improve the efficiency of the IEM under large-scale RES penetration, and promote the truthful declarations of market participants by applying a Vickrey-Clarke-Groves (VCG) auction scheme to the IEM, and establishes a two-stage IEM model that promotes compatibility between the incentives of market participants to enhance market fairness. The present study also addresses the imbalance between market revenue and expenditure typically produced by the VCG auction scheme by designing an ex-post payment redistribution mechanism to ensure the equitable cost recovery of all market participants. Simulation results demonstrate that the application of the proposed VCG auction system to the IEM ensures maximum efficiency, cost recovery, and incentive compatibility as dominant strategies, and helps to integrate large-scale RES penetration with the IEM.

INDEX TERMS Regional integrated energy system, integrated energy market, incentive compatibility, VCG auction, renewable energy system.

NUMENCLATURE

A. INDICES

i, j, k	Subscript indices of buses in a distributed electric system (DES).
m, n	Subscript indices of nodes in a distributed gas system (DGS).
u, v, w	Subscript indices of nodes in a distributed heating system (DHS).
d	Subscript index of a heat demand.
S	Subscript index of a heat source.
t	Subscript index of a discrete time period.
min	Superscript index of a minimum value.
max	Superscript index of a maximum value.
π	Superscript index of an energy requirement scenario.
0	Superscript index of a day-ahead stage.
s	Superscript index of a real-time stage.
J	Subscript index of an energy producer (EP).
K	Subscript index of an energy load (EL).
α	Subscript index of a market participant.

B. SETS

Ω_{MCT}	Set of micro coal-fired turbines (MCTs).
Ω_{MGT}	Set of micro gas-fired turbines (MGTs).
Ω_{HB}	Set of heating boilers (HBs).
Ω_{Le}	Set of electric demands.
Ω_{Lg}	Set of gas demands.

The associate editor coordinating the review of this article and approving it for publication was Xianming Ye.

Ω_{Lh} Set of heat demands.
Ω_{EL} Set of ELs.
Ω_{EP} Set of EPs.
Ξ_{EL} Set of ELs excluding EL K.
Ξ_{EP} Set of EPs excluding EP J.

C. VARIABLES

$\mathbf{R}$	Expected social welfare.
$\mathbf{S}$	The charges for the EL K/the payment to EP J
F	Objective function under the locational marginal price mechanism.
F^0	Day-ahead stage cost.
F^S	Real-time stage cost.
F^U	Total utility of energy demands.
P_{MCT}	Active power generation of MCTs (p.u.).
Q_{MCT}	Reactive power generation of MCTs (p.u.).
P_{EG}	Active power from external electrical power grids(p.u.).
Q_{EG}	Reactive power from external electrical power grids(p.u.
Q_{NG}	Gas production of gas sources (p.u.).
Q_{HB}	Heat supply of HBs (p.u.).
R^U_{MCT}	Upward reserve capacity of MCTs (p.u.).
R^D_{MCT}	Downward reserve capacity of MCTs (p.u.).
R^U_{HB}	Upward reserve capacity of HBs (p.u.).
R^D_{HB}	Downward reserve capacity of HBs (p.u.).
R^U_{NG}	Upward reserve capacity of gas sources (p.u.).
R^D_{NG}	Downward reserve capacity of gas sources (p.u.).
P_{Le}, Q_{Le}	Active/reactive electric demand (p.u.).
Q_{Lg}, Q_{Lh}	Gas/heat demand (p.u.).
p_π	The probability of the π-th scenario.
$\alpha_e, \alpha_g, \alpha_h$	Access ratio of electric/gas/heat demand (p.u.).
r^U_{MCT}	Upward balancing regulation of MCTs (p.u.).
r^D_{MCT}	Downward balancing regulation of MCTs (p.u.).
r^U_{HB}, r^D_{HB}	Upward/downward balancing regulation of HBs (p.u.).
r^U_{NG}, r^D_{NG}	Upward/downward balancing regulation of gas sources (p.u.).
P_{MGT}	Power generation of MGTs (p.u.).
P_{CHP}	Power generation of combined heat and power (CHP) units (p.u.).
P_{ij}, Q_{ij}	Active/reactive power flow through branch $i-j$ (p.u.).
I_{ij}	Squared current magnitude through branch $i-j$ (p.u.).
U_i	Squared voltage of electrical bus i (p.u.).
F_S	Gas production of gas generation (p.u.).
F_{MGT}	Gas consumption of MGTs (p.u.).
F_{CHP}	Gas consumption of CHP units (p.u.).
F_{mn}	Gas flow through pipeline $m-n$ (p.u.).
Π_m	Squared gas pressure of node m (p.u.).
T_κ, T_υ	Inlet/outlet temperature of a pipeline.
T_e	Ambient temperature.
T_v	Temperature of node v (p.u.).
L_{uv}, f_{uv}	Length/flow rate of pipeline $u-v$ (p.u.).
T_{LS}, T_{LR}	Temperature at the supply/return side of loads (p.u.).
T_κ, T_υ	Inlet/outlet temperature of a pipeline.
T_{HS}, T_{HR}	Temperature at the supply/return side of heat sources (p.u.).
Q_H	Output of heat sources (p.u.).
λ_{sp}	Curtailment rates of renewable energy source (RES) generation (p.u.).
S_{BI}	The value of budget imbalance in the IEM.

D. PARAMETERS

C_{MCT}	MCT cost (mu).
C_{NG}	Natural gas cost (mu).
C_{HB}	HB cost (mu).
C^U_{MCT}	Upward reserve cost of MCTs (mu)
C^D_{MCT}	Downward reserve cost of MCTs (mu)
C^U_{HB}	Upward reserve cost of HBs (mu)
C^D_{HB}	Downward reserve cost of HBs
C^U_{NG}	Upward reserve cost of gas sources (mu).
C^D_{NG}	Downward reserve cost of gas sources (mu).
V_e, V_g, V_h	Electricity/gas/heat demand shedding cost (mu).
L_e, L_g, L_h	Utility of electric/gas/heat demand (mu).
P_{RES}	Dispatched RES generation (p.u.).
r_{ij}, x_{ij}	Resistance/reactance of branch i-j (p.u.).
C_{mn}	Weymouth constant of pipeline m-n (p.u.).
R, c, ρ	Specific thermal resistance of pipelines/specific heat of water/density of water (mu).
η_{HX}	Average efficiency of heat exchange equipment (mu).
η_{MGT}	Conversion efficiency of MGTs (mu).
η_{CHP}	Conversion efficiency of CHP units (mu).
η_{Ce}, η_{Ch}	Electric/heat production efficiency of CHP units (mu).

I. INTRODUCTION

Regional integrated energy systems (RIESs) are an important physical carrier of the energy internet that promises the integrated delivery of energy and information. Here, an RIES integrates multiple energy sources on a regional scale, and may include a distributed electric system (DES), a distributed heating system (DHS), a distributed gas system (DGS), and energy converters (ECs) such as combined heating and power (CHP) units that convert natural gas into electricity and heat, and micro gas turbines (MGTs) that convert natural gas to electrical power. The integration of multiple energy sources by an RIES takes advantage of the coupling characteristics

of these various sources in space and time to realize their complementary utilization, and to provide new solutions for addressing energy shortages [1]. One or more RIESs and market participants together form an integrated energy market (IEM). These market participants include integrated energy market operators (IEMO), energy producers (EPs), and energy loads (ELs). The day-ahead market is conducted on the day prior to energy delivery. Here, an IEMO clears the IEM based on the production marginal cost provided by the EPs and the next-day energy demands provided by the ELs to schedule production and consumption levels and day-ahead market-clearing prices [2] to settle the IEM. Meanwhile, sufficient reserve capacity is prepared to accommodate possible uncertainties in real-time operation efficiently in accordance with the real-time market, which occurs in the period prior to energy delivery and is the market mechanism that balances production and consumption. As such, the development of RIESs is closely linked with the establishment of IEMs, which are conducive to the fair distribution of production resources and the friendly interaction between EPs and energy consumers [3]. Accordingly, many countries have presently begun to develop pilot IEMs, and the related market systems and mechanisms have been continuously improved. Nordic countries in particular, such as Finland and Sweden, have highly developed IEMs, which have effectively solved the price monopoly problem [3]. The practical experience of the IEM implemented in Quebec, Canada has demonstrated that the close combination of electricity, natural gas, and thermal markets can effectively promote reductions in energy consumption and the emissions of harmful gases [4]. The Chinese government has also begun to actively implement a pilot IEM to promote the marketization of energy trading in China.

Most existing IEM settlement and trading mechanisms employed worldwide are based on the spot market, which functions according to a perfect competition model where the locational marginal price (LMP) is adopted for market clearing [5]. However, both theory and practice have demonstrated that the LMP mechanism generally fails to promote the declaration of truthful marginal costs by market participants in the process of clearing and settlement of the IEM. Here, tense market supply and demand relationships or line congestions provide EPs with economic incentives to present falsely high marginal cost quotes to increase the LMP, and thereby increase their profits [6]. Naturally, this type of behavior stems from the incompatible incentives of the market participants that undermine fair competition, and will ultimately have a negative impact on market efficiency by changing the economic distribution of dispatching and reducing social welfare [6]–[9].

The above-discussed problem has been addressed by efforts to develop incentive compatibility strategies to create market conditions whereby the truthful performance of market participants represents their optimal strategy to realize the maximization of their individual interests rationally. This is consistent with the outcomes of strategies developed in the field of mechanism design, such as the Vickrey-Clarke-Groves (VCG) auction strategy [10]. At present, many scholars have studied the implementation of incentive compatibility via VCG auction. For example, the respective market clearing results based on VCG and LMP have been analyzed and compared [11]. Applying VCG auction to the electricity market has been demonstrated to improve the economic benefits of EPs [12]. Moreover, VCG auction has also been demonstrated to be applicable to the storage of energy, such as for ensuring the truthful declaration of battery energy storage parameters [13].

The impact of renewable energy sources (RESs) such as wind power and photovoltaic arrays on the functionality of IEMs is another problematic issue. For example, RES participation in IEMs is commonly implemented using feed-in tariffs (FIT), whose prices are currently set by government departments and related companies, and the uncertainty of RES output owing to random variations in, e.g., wind speed and cloud cover is often not considered [14]. However, the impact of RES output uncertainty on the IEM can be neglected only if the level of RES penetration is limited because this impact becomes increasingly obvious and more complex as the level of RES penetration increases, which ultimately affects the operating costs of IEMs and the economic benefits of market participants. In addition, the uncertainty of RES output further increases the power reserve capacity requirements of RIESs to meet load demands under possible extreme fluctuations in RES power production. Here, two-stage stochastic dispatch, which divides the power dispatch problem into day-ahead energy-reserve dispatch and real-time operation, has been demonstrated to be capable of effectively addressing the impact of RES output uncertainty on RIES operations [2]. Moreover, the energy supply plan made in the day-ahead market can be adjusted in the real-time market according to two-stage stochastic dispatch in real time, which can ensure better adaptation of an IEM to the uncertainty of RES output and improve market efficiency [15]. The impacts of demand and supply uncertainties on the optimal design of RIESs have also been investigated systematically [16]–[18]. Meanwhile, two-stage dispatch has been applied for facilitating electric power distribution decisions regarding grid purchase, generation unit dispatching, and interruptible load scheduling [19].

In this paper, we apply an incentive-compatible mechanism based on VCG auction to improve the efficiency of IEM operations in both the day-ahead and real-time markets (i.e., two-stage IEM) under high RES penetration. The present work makes the following contributions.

1) A convex two-stage stochastic programming model of an RIES is established to determine RIES production and consumption levels, and arrange the energy reserve capacity. The impact of RES output uncertainty on the RIES is appropriately predicted to achieve economic system operation.
2) The VCG auction mechanism is applied to a two-stage IEM model to motivate market participants to

declare truthful marginal costs. Then, the incentive compatibility of the scheme was proved. The theory was proved that the mechanism satisfies the dominant strategy incentive compatibility, which can effectively stimulate the EPs to report the cost truthfully.

3) The VCG auction scheme can result in budget deficits for IEMOs that should be exogenously recovered based on additional payments from market participants [20]. Therefore, we quantify budget imbalances of IEM as positive and negative, and propose an ex-post mechanism to partially recover revenue adequacy. Here, positive and negative budget imbalances are respectively redistributed by proportionally rewarding and charging market participants for their contributions toward the corresponding budget imbalance.

Accordingly, the application of the proposed VCG auction scheme to the IEM ensures maximum efficiency, cost-recovery, and incentive-compatibility as dominant strategies, and helps to integrate large-scale RES penetration with the IEM. These benefits of the proposed development are verified based on simulations employing two different test conditions involving changing heat demands and varying RES penetrations for a realistic RIES.

The remainder of the paper is organized as follows. Section II describes the IEM framework and the model assumptions. Sections III and IV establish the LMP mechanism for the two-stage IEM, and the VCG auction mechanism, respectively. Section V presents the simulation case studies considering multiple conventional and wind power EPs that compete in the IEM. Finally, Section VI concludes the paper.

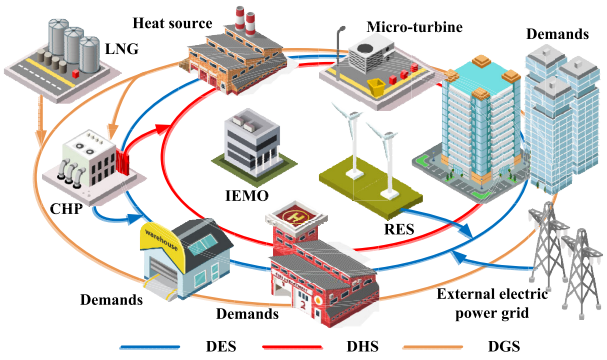

FIGURE 1. Schematic illustrating a city-scale RIES and a corresponding IEM framework.

II. MARKET FRAMEWORK AND MODEL ASSUMPTIONSS

A. MARKET FRAMEWORK

The main research object of this paper is the typical city-scale RIES illustrated in Fig. 1. The RIES consists of a DES, a DHS, a DGS, and ECs. The DES obtains and transmits electrical power derived from local electrical power generation units (such as RESs, which are here denoted by a single wind farm), external (i.e., non-local) electrical power grids, and ECs. The DGS purchases natural gas directly from liquid natural gas (LNG) facilities to meet its natural gas supply needs. The heat energy required for the DHS derives from local heating equipment (such as heating boilers; HBs). According to Fig. 1, we consider stochastic and deterministic EPs in the IEM, where stochastic EPs are associated with RESs and deterministic EPs are associated with conventional power production devices such as MGTs. As discussed, an IEMO clears the IEM in the day-ahead market. However, another important responsibility of an IEMO is to plan the energy reserves of the RIES and adjust the system in real time the following day to cope with the uncertainty of RES output.

B. RIES MODEL ASSUMPTIONS

The primary model assumptions in this paper are described as the follows.

1) The more rigorous non-convex and nonlinear RIES model is not conducive toward obtaining solutions of the LMP. Therefore, we employ a linearized RIES model, where the second-order cone (SOC) relaxation method is applied to relax the nonlinear DES and DGS equations to obtain linear forms [15]. We also apply a widely used model of a DHN under a constant flow and variable temperature (CF-VT) control strategy [21].
2) The load demands of the ELs are considered to be deterministic because these are much less stochastic than RES output. Stochastic scenario modeling, where each scenario has a corresponding probability of occurrence, is applied to describe the uncertainty of RES output in the real-time market.
3) The outputs of the RESs are considered to be ostensibly controlled by utility companies, and their marginal cost is zero [22]. In addition, all RESs (i.e., wind farms) are at all times subject to an equivalent wind speed.

III. TWO-STAGE MARKET BASED LMP MECHANISM

The first step of the proposed approach for enforcing incentive compatibility in the IEM is to ensure efficient economic dispatch by clearing the two-stage IEM model based LMP mechanism, which guarantees market efficiency under an assumption of a perfectly competitive market. In the proposed two-stage IEM model, all market participants are included. All participants are considered to be price-takers and submit their true cost/utility to the IEMO. As such, we assume a perfectly competitive market.

A. OBJECTIVE FUNCTION

The two-stage IEM clearing process is based on the LMP, and takes the maximization of social welfare as the objective function. Here, we define the total social welfare as follows:

$$\mathbf{R}\,[SW] = \sum_{t=1}^{24} \mathbf{R}\,[SW]_t = \sum_{t=1}^{24} \left[F_t^U - \left(F_t^0 + F_t^S \right) \right]. \quad (1)$$

However, optimization problems are generally defined as minimization problems. Therefore, we convert objective

function (1) to reflect a minimization of the negative total social benefit [9]:

$$\min\ F = -\mathbf{R}\left[SW\right] = \left(F^0 + F^S\right) - F^U. \tag{2}$$

where F^0 includes the energy and reserve capacity costs as follows.

$$F^0 = \underbrace{\sum_{t=1}^{24}\left(\begin{array}{l}\sum\limits_{i\in\Omega_{MCT}} C_{MCT,i}P^0_{MCT,i,t} + C_{NG}Q^0_{NG,t} \\ +\sum\limits_{u\in\Omega_{HB}} C_{HB,u}Q^0_{HB,u,t}\end{array}\right)}_{Day-ahead\ energy\ costs} + \underbrace{\sum_{t=1}^{24}\left[\begin{array}{l}\sum\limits_{i\in\Omega_{MCT}}\left(C^U_{MCT,i}R^U_{MCT,i,t} + C^D_{MCT,i}R^D_{MCT,i,t}\right) \\ +\sum\limits_{u\in\Omega_{HB}}\left(C^U_{HB,u}R^U_{HB,u,t} + C^D_{HB,u}R^D_{HB,u,t}\right) \\ +\left(C^U_{NG}R^U_{NG,t} + C^D_{NG}R^D_{NG,t}\right)\end{array}\right]}_{Reserve\ capacity\ costs} \tag{3}$$

In addition, F^S includes energy redispatch and load shedding costs as follows.

$$F^S = \underbrace{\sum_{t=1}^{24}\sum_{\pi=1}^{\pi\max} p_\pi\left[\begin{array}{l}\sum\limits_{i\in\Omega_{Le}} V_e\left(\alpha^0_{e,i,t} - \alpha^{s,\pi}_{e,i,t}\right)P_{Le,i,t} \\ +\sum\limits_{m\in\Omega_{Lg}} V_g\left(\alpha^0_{g,m,t} - \alpha^{s,\pi}_{g,m,t}\right)Q_{Lg,m,t} \\ +\sum\limits_{u\in\Omega_{Lh}} V_h\left(\alpha^0_{h,u,t} - \alpha^{s,\pi}_{h,u,t}\right)Q_{Lh,u,t}\end{array}\right]}_{Banlancing\ costs(load shedding\ costs)} + \underbrace{\sum_{t=1}^{24}\sum_{\pi=1}^{\pi\max} p_\pi\left[\begin{array}{l}\sum\limits_{i\in\Omega_{MCT}} C_{MCT,i}\left(r^{U,\pi}_{MCT,i,t} - r^{D,\pi}_{MCT,i,t}\right) \\ +\sum\limits_{u\in\Omega_{HB}} C_{HB,u}\left(r^{U,\pi}_{HB,u,t} - r^{D,\pi}_{HB,u,t}\right) \\ +C_{NG}\left(r^{U,\pi}_{NG,t} - r^{D,\pi}_{NG,t}\right) + P^{s,\pi}_{EG,j,t}\end{array}\right]}_{Banlancing\ costs(energy\ redispatch)} \tag{4}$$

Finally, F^U in (2) can be expressed as follows.

$$F^U = \sum_{t=1}^{24}\left(\begin{array}{l}\sum\limits_{i\in\Omega_{Le}} L_{Le,i}\alpha^0_{Le,i,t}P_{Le,i,t} \\ +\sum\limits_{m\in\Omega_{Lg}} L_{Lg,m}\alpha^0_{Lg,m,t}Q_{Lg,m,t} \\ +\sum\limits_{u\in\Omega_{Lh}} L_{Lh,u}\alpha^0_{Lh,u,t}P_{Lh,u,t}\end{array}\right) \tag{5}$$

B. DAY-AHEAD MARKET

The DES model in day-ahead market is given as follows.

$$\begin{aligned} &P^0_{EG,j,t} + P^0_{MCT,j,t} + P^0_{MGT,j,t} + P^0_{RES,j,t} + P^0_{CHP,j,t} \\ &\quad + \sum_{i\in j}\left(P^0_{ij,t} - I^0_{ij,t}r_{ij}\right) \\ &\quad = \alpha^0_{e,j,t}P_{Le,j,t} + \sum_{k\in j} P^0_{jk,t} \end{aligned} \tag{6}$$

$$\begin{aligned} &\sum_{i\in j}\left(Q^0_{ij,t} - I^0_{ij,t}x_{ij}\right) \\ &\quad = \alpha^0_{e,j,t}Q^0_{Le,j,t} - Q^0_{EG,j,t} \\ &\quad\quad + \sum_{i\in j} Q^0_{ij,t} - Q^0_{MCT,j,t} \end{aligned} \tag{7}$$

$$\begin{aligned} U^0_{j,t} - U^0_{i,t} &= -2\left(P^0_{ij,t}r_{ij} + Q^0_{ij,t}x_{ij}\right) \\ &\quad + I^0_{ij,t}\left(r^2_{ij} + x^2_{ij}\right) \end{aligned} \tag{8}$$

$$U^0_{i,t}I^0_{ij,t} = \left(P^0_{ij,t}\right)^2 + \left(Q^0_{ij,t}\right)^2 \tag{9}$$

$$0 \le \alpha^0_{e,j,t} \le 1 \tag{10}$$

$$P^{\min}_{MCT} \le P^0_{MCT,j,t} \le P^{\max}_{MCT} \tag{11}$$

$$Q^{\min}_{MCT} \le Q^0_{MCT,j,t} \le Q^{\max}_{MCT} \tag{12}$$

$$P^{\min}_{ramp} \le P^0_{MCT,j,t} - P^0_{MCT,j,t-1} \le P^{\max}_{ramp} \tag{13}$$

$$U^{\min}_j \le U^0_{j,t} \le U^{\max}_j \tag{14}$$

$$I^{\min}_{ij} \le I^0_{ij,t} \le I^{\max}_{ij} \tag{15}$$

$$R^{U,\min}_{MCT} \le R^U_{MCT,j,t} \le R^{U,\max}_{MCT} \tag{16}$$

$$R^{D,\min}_{MCT} \le R^D_{MCT,j,t} \le R^{D,\max}_{MCT} \tag{17}$$

$$\begin{aligned} &P^0_{MCT,j,t} + R^D_{MCT,j,t} \\ &\quad \le P^{\max}_{MCT} \end{aligned} \tag{18}$$

$$0 \le P^0_{MCT,j,t} - R^U_{MCT,j,t} \tag{19}$$

Here, (6) and (7) represent the active and reactive power flow equations of bus j, respectively. The relationships between the bus voltage, the branch flows, and the current are represented in (8) and (9), respectively. The inequality constraints of the DES are presented in (10)-(15), which include DGS output constraints, voltage constraints, and line constraints. The reserve capacity constraints are presented in (16)-(19). In addition, the non-convex equation (9) can be transformed into the form of a convex equation represented in (20) by SOC relaxation, which can be expressed in the standard form given by (21) [15].

$$\begin{aligned} \left(P^0_{ij,t}\right)^2 + \left(Q^0_{ij,t}\right)^2 &\le I^0_{ij,t}U^0_{i,t} \\ \Rightarrow \left(2P^0_{ij,t}\right)^2 + \left(2Q^0_{ij,t}\right)^2 &+ \left(I^0_{ij,t} - U^0_{i,t}\right)^2 \\ &\le \left(I^0_{ij,t} + U^0_{i,t}\right)^2 \end{aligned} \tag{20}$$

$$\left\|\begin{array}{c}2P^0_{ij,t} \\ 2Q^0_{ij,t} \\ I^0_{ij,t} - U^0_{i,t}\end{array}\right\|_2 \le I^0_{ij,t} + U^0_{i,t} \tag{21}$$

The DGS model is given as follows.

$$\begin{aligned} &F^0_{S,m,t} - F^0_{MGT,m,t} - F^0_{CHP,m,t} \\ &\quad = \sum_{n\in m} F^0_{mn,t} + \alpha^0_{Lg,m,t}Q_{Lg,m,t} \end{aligned} \tag{22}$$

$$\left(F^0_{mn,t}\right)^2 = C^2_{mn}\left(\Pi^0_{m,t} - \Pi^0_{n,t}\right) \tag{23}$$

$$Q^0_{NG,t} = \sum_{m\in\Omega_{GS}} F^0_{S,m,t} \tag{24}$$

$$0 \le \alpha^0_{g,m,t} \le 1 \tag{25}$$

$$\Pi^{\min}_m \le \Pi^0_{m,t} \le \Pi^{\max}_m \tag{26}$$

$$F^{\min}_S \le F^0_{S,m,t} \le F^{\max}_S \tag{27}$$

$$F^{\min}_{ramp} \le F^0_{S,m,t} - F^0_{S,m,t-1} \le F^{\max}_{ramp} \tag{28}$$

$$R^{U,\min}_{NG} \le R^U_{NG,t} \le R^{U,\max}_{NG} \tag{29}$$

$$R^{D,\min}_{NG} \le R^D_{NG,t} \le R^{D,\max}_{NG} \tag{30}$$

$$Q^0_{NG,t} + R^D_{NG,t} \le Q^{\max}_{NG} \tag{31}$$

$$0 \le Q^0_{NG,t} - R^U_{NG,t} \tag{32}$$

Here, (22) represents the node flow balance equation and (23) represents the relationship between node air pressure and pipeline flow. The natural gas supply equation is given in (24), and (25)-(32) are the inequality constraints of the DGS. The relationship between the node pressure and the flow rate shown in (23) is non-convex, and can be transformed into the form of a convex equation represented in (33) by SOC relaxation, where the standard form is given in (34) [15].

$$\begin{aligned}\left(F^0_{mn,t}\right)^2 &\le C^2_{mn}\left(\Pi^0_{m,t} - \Pi^0_{n,t}\right)\\ &\Rightarrow \left(\frac{2F^0_{mn,t}}{C_{mn}}\right)^2 + \left(\Pi^0_{m,t} - \Pi^0_{n,t} - 1\right)^2\\ &\le \left(\Pi^0_{m,t} - \Pi^0_{n,t} + 1\right)^2 \end{aligned} \tag{33}$$

$$\left\| \begin{matrix} 2F^0_{mn,t}/C_{mn} \\ \Pi^0_{m,t} - \Pi^0_{n,t} - 1 \end{matrix} \right\|_2 \le \left(\Pi^0_{m,t} - \Pi^0_{n,t} + 1\right) \tag{34}$$

Finally, the CF-VT model of the DHS can be expressed as follows.

$$T^0_{\kappa v,t} - T^0_{\upsilon u,t} = \left(T_{e,t} - T^0_{\upsilon u,t}\right)\frac{L_{uv}}{Rc\rho f_{uv}} \tag{35}$$

$$\sum_{u\in v} f_{uv} = \sum_{w\in v} f_{vw} \tag{36}$$

$$\sum_{u\in v} T^0_{\kappa v,t} f_{uv} = T^0_{\upsilon v,t}\sum_{w\in v} f_{vw} \tag{37}$$

$$T^0_{\upsilon v,t} = T^0_{v,t} \tag{38}$$

$$\alpha^0_{h,m,t} P_{Lh,d,t} = c\rho\eta_{HX} f\left(T^0_{LS,d,t} - T^0_{LR,d,t}\right) \tag{39}$$

$$Q^0_{H,S,t} = c\rho\eta_{HX} f\left(T^0_{HS,S,t} - T^0_{HR,S,t}\right) \tag{40}$$

$$Q^0_{H,S,t} = \sum_{u\in\Omega_{HB}} Q^0_{HB,u,t} \tag{41}$$

$$Q^0_{H,S,t} = \sum_{u\in\Omega_{CHP}} Q^0_{CHP,u,t} \tag{42}$$

$$0 \le \alpha^0_{h,m,t} \le 1 \tag{43}$$

$$T^{\min}_u \le T^0_{u,t} \le T^{\max}_u \tag{44}$$

$$T^{\min}_{LS,d,t} \le T^0_{LS,d,t} \le T^{\max}_{LS,d,t} \tag{45}$$

$$T^{\min}_{HS} \le T^0_{HS,s,t} \le T^{\max}_{HS} \tag{46}$$

$$R^{U,\min}_{HB} \le R^U_{HB,u,t} \le R^{U,\max}_{HB} \tag{47}$$

$$R^{D,\min}_{HB} \le R^D_{HB,u,t} \le R^{D,\max}_{HB} \tag{48}$$

$$Q^0_{HB,u,t} + R^D_{HB,u,t} \le Q^{\max}_{HB} \tag{49}$$

$$0 \le Q^0_{HB,u,t} - R^U_{HB,u,t} \tag{50}$$

In addition, the constraints of the EC devices can be expressed as follows.

$$P^0_{MGT,i,t} = \eta_{MGT} F^0_{MGT,m,t} \tag{51}$$

$$F^0_{CHP,t}\eta_{CHP} = \eta_{CHP,e} P^0_{CHP,i,t} + \eta_{CHP,h} Q^0_{CHP,u,t} \tag{52}$$

$$P^{\min}_{MGT} \le P^0_{MGT,i,t} \le P^{\max}_{MGT} \tag{53}$$

Here, (51) and (53) are the operational constraints of the MGTs, and (52) is the operational constraint of the CHP units [23].

C. REAL-TIME MARKET

Because the energy reserve was determined according to the submitted plans of the market participants, the uncertainty of RES output was not considered, and the production levels of the stochastic EPs cannot be accurately predicted before the day-ahead market closes. Therefore, an IEMO must adjust the market in real time to balance its clearing price. In this subsection, the real-time market constraints that are equivalent to those of the day-ahead market are not repeated. All non-redundant constraints of the real-time market are given as follows.

$$\begin{aligned} P^{s,\pi}_{EG,j,t} &+ \left(P^0_{MCT,j,t} + r^{U,\pi}_{MCT,j,t} - r^{D,\pi}_{MCT,j,t}\right)\\ &+ P^{s,\pi}_{MGT,j,t} + P^{s,\pi}_{CHP,j,t}\\ &+ P^0_{RES,j,t}\left(1 - \lambda^{\pi}_{sp,j,t}\right)\\ &- \sum_{k\in j} P^{s,\pi}_{jk,t}\\ + \sum_{i\in j}\left(P^{s,\pi}_{ij,t} - I^{s,\pi}_{ij,t} r_{ij}\right) &= \left(\alpha^0_{e,j,t} - \alpha^{s,\pi}_{e,j,t}\right) P_{Le,j,t} \end{aligned} \tag{54}$$

$$\begin{aligned} \sum_{i\in j}\left(Q^{s,\pi}_{ij,t} - I^{s,\pi}_{ij,t} x_{ij}\right) &+ Q^{s,\pi}_{MCT,j,t} - \sum_{i\in j} Q^{s,\pi}_{ij,t}\\ -Q^{s,\pi}_{EG,j,t} &= \left(\alpha^0_{e,j,t} - \alpha^{s,\pi}_{e,j,t}\right) Q_{Le,j,t} \end{aligned} \tag{55}$$

$$\begin{aligned} U^{s,\pi}_{j,t} - U^{s,\pi}_{i,t} &= -2\left(P^{s,\pi}_{ij,t} r_{ij} + Q^{s,\pi}_{ij,t} x_{ij}\right)\\ &+ I^{s,\pi}_{ij,t}\left(r^2_{ij} + x^2_{ij}\right) \end{aligned} \tag{56}$$

$$\left\| \begin{matrix} 2P^{s,\pi}_{ij,t} \\ 2Q^{s,\pi}_{ij,t} \\ I^{s,\pi}_{ij,t} - U^{s,\pi}_{i,t} \end{matrix} \right\|_2 \le I^{s,\pi}_{ij,t} + U^{s,\pi}_{i,t} \tag{57}$$

$$0 \le r^{U,\pi}_{MCT,i,t} \le R^U_{MCT,i,t} \tag{58}$$

$$0 \le r^{D,\pi}_{MCT,i,t} \le R^D_{MCT,i,t} \tag{59}$$

$$0 \le \alpha^{s,\pi}_{e,j,t} \le \alpha^0_{e,j,t} \tag{60}$$

$$\begin{aligned} F^{s,\pi}_{S,m,t} - F^{s,\pi}_{MGT,m,t} - F^{s,\pi}_{CHP,m,t} &- \sum_{n\in m} F^{s,\pi}_{mn,t}\\ &= \alpha^{s,\pi}_{g,m,t} Q_{Lg,m,t} \end{aligned} \tag{61}$$

$$Q^{0}_{NG,t} + r^{U,\pi}_{NG,t} - r^{D,\pi}_{NG,t} = \sum_{m\in\Omega_{GS}} F^{s,\pi}_{S,m,t} \tag{62}$$

$$0 \le \alpha^{s,\pi}_{g,m,t} \le \alpha^{0}_{g,m,t} \tag{63}$$

$$\left\| \begin{matrix} 2F^{s,\pi}_{mn,t}/C_{mn} \\ \Pi^{s,\pi}_{m,t} - \Pi^{s,\pi}_{n,t} - 1 \end{matrix} \right\|_2 \le \left(\Pi^{s,\pi}_{m,t} - \Pi^{s,\pi}_{n,t} + 1\right) \tag{64}$$

$$T^{s,\pi}_{\kappa v,t} - T^{s,\pi}_{\upsilon u,t} = \left(T_{e,t} - T^{s,\pi}_{\upsilon u,t}\right)\frac{L_{uv}}{Rc\rho f_{uv}} \tag{65}$$

$$\sum_{u\in v} T^{s,\pi}_{\kappa v,t} f_{uv} = T^{s,\pi}_{\upsilon v,t} \sum_{w\in v} f_{vw} \tag{66}$$

$$T^{s,\pi}_{\upsilon v,t} = T^{s,\pi}_{v,t} \tag{67}$$

$$\alpha^{s,\pi}_{h,m,t} P_{Lh,d,t} = c\rho\eta_{HX} f\left(T^{s,\pi}_{LS,d,t} - T^{s,\pi}_{LR,d,t}\right) \tag{68}$$

$$Q^{s,\pi}_{H,S,t} = c\rho\eta_{HX} f\left(T^{s,\pi}_{HS,S,t} - T^{s,\pi}_{HR,S,t}\right) \tag{69}$$

$$Q^{s,\pi}_{H,S,t} = Q^{0}_{HB,u,t} + r^{U,\pi}_{HB,u,t} - r^{D,\pi}_{HB,u,t} \tag{70}$$

$$0 \le \alpha^{s,\pi}_{h,m,t} \le \alpha^{0}_{h,m,t} \tag{71}$$

$$P^{s,\pi}_{MGT,i,t} = \eta_{MGT} F^{s,\pi}_{MGT,m,t} \tag{72}$$

$$F^{s,\pi}_{CHP,t}\eta_{CHP} = \eta_{Ce} P^{s,\pi}_{CHP,i,t} + \eta_{Ch} Q^{s,\pi}_{CHP,u,t} \tag{73}$$

Here, (54)-(60) are the DES constraints, (61)-(64) are the DGS constraints, (65)-(70) are the DHS constraints, and (71)-(73) are the EC constraints.

D. SOLUTION METHODOLOGY

A two-stage IEM model based on LMP clearing can be expressed as follows.

$$\min_{x^0_e, x^0_d, y^{s,\pi}_e} \sum_{t=1}^{24} \left\{ \begin{matrix} \sum_{\pi\in\Omega_\pi} \left[\begin{matrix} \sum_{e\in\Omega_{EP}} C_e\left(x^0_{e,t}, y^{s,\pi}_{e,t}\right) + \\ \sum_{d\in\Omega_D} V_d\left(y^{s,\pi}_{d,t}\right) \end{matrix} \right] \\ + \sum_{e\in\Omega_{EP}} C_e\left(x^0_{e,t}\right) - \sum_{d\in\Omega_D} L_d\left(x^0_{d,t}\right) \end{matrix} \right\} \tag{74}$$

where x^0_e and x^0_d are the variable vectors of EPs and ELs in day-ahead market. $y^{s,\pi}_e$ and $y^{s,\pi}_d$ are the variable vectors of EPs and ELs in real-time market. C_e, V_d and L_d are the parameter vectors of energy cost, load shedding costs and demands utility. The (74) is subject to the following respective equality and inequality constraints.

$$h\left(x^0_t, y^{s,\pi}_t\right) = 0 \tag{75}$$

$$g\left(x^0_t, y^{s,\pi}_t\right) \le 0 \tag{76}$$

The model represented by (74)-(76) is an SOC optimization problem, and it is essentially a convex problem. The optimality of the solution and the computational efficiency have excellent characteristics [25]. Existing SOC optimization algorithms can easily solve difficult nonlinear problems [26]. In this paper, the model is solved using the MOSEK solver in GAMS running on a personal computer with an Intel Core 2.8 GHz CPU and 8 GB of RAM.

IV. INCENTIVE-COMPATIBLE MARKET UNDER THE VCG MECHANISM

The second step of the proposed approach applies the VCG auction strategy, which reflects the economic impact of each participant on social welfare by demanding charges from ELs and determining payments to EPs based on their individual contributions toward maximizing the social welfare. Note that VCG auction ensures a perfectly competitive IEM, through a payment scheme which aligns the objectives of individual participants with the maximization of social welfare.

A. VCG PAYMENTS TO EPS

Here, we calculate the revenue of the J-th EP. The social welfare when J does not participate in the IEM is derived from the solution of the following optimization problem.

$$\min_{x^0_e, x^0_d, y^{s,\pi}_e} \sum_{t=1}^{24} \left\{ \begin{matrix} \sum_{\pi\in\Omega_\pi} \left[\begin{matrix} \sum_{e\in\Xi_{EP}} C_e\left(x^0_{e,t}, y^{s,\pi}_{e,t}\right) + \\ \sum_{d\in\Omega_D} V_d\left(y^{s,\pi}_{d,t}\right) \end{matrix} \right] \\ + \sum_{e\in\Xi_{EP}} C_e\left(x^0_{e,t}\right) - \sum_{d\in\Omega_D} L_d\left(x^0_{d,t}\right) \end{matrix} \right\} \tag{77}$$

Meanwhile, J is excluded from constraints (75) and (76). The solution to (77) is then employed in (2) to obtain the total social welfare $\mathbf{R}[SW_{-J}]_t$ corresponding to the time period t when J does not participate in the IEM. This process is repeated for each EP by excluding one EP at a time. Finally, the payment to EP J is given as

$$\mathbf{S}_{J,t} = \mathbf{R}\left[SW_J\right]_t + C_J\left(x^0_{J,t}\right) - \mathbf{R}\left[SW_{-J}\right]_t. \tag{78}$$

Each EP's settlement is defined according to the cost submission of other EPs and its own mentioned benefits, so the EP has no incentive to falsely report high cost.

B. VCG PAYMENTS TO ELS

Next, we calculate the charges for the consumption of the K-th EL. The social welfare when K does not participate in the IEM is derived from the solution of the following optimization problem.

$$\min_{x^0_e, x^0_d, y^{s,\pi}_e} \sum_{t=1}^{24} \left\{ \begin{matrix} \sum_{\pi\in\Omega_\pi} \left[\begin{matrix} \sum_{e\in\Omega_{EP}} C_e\left(x^0_{e,t}, y^{s,\pi}_{e,t}\right) + \\ \sum_{d\in\Xi_D} V_d\left(y^{s,\pi}_{d,t}\right) \end{matrix} \right] \\ + \sum_{e\in\Omega_{EP}} C_e\left(x^0_{e,t}\right) - \sum_{d\in\Xi_D} L_d\left(x^0_{d,t}\right) \end{matrix} \right\} \tag{79}$$

Meanwhile, K is excluded from constraints (75) and (76). The solution to (79) is then employed in (2) to obtain the total social welfare $\mathbf{R}[SW_{-K}]_t$ corresponding to the time period t when K does not participate in the IEM. This process is repeated for each EL by excluding one EL at a time. Finally, the charges for the consumption of K is give as

$$\mathbf{S}_{K,t} = [SW_{-K}]_t - \left\{[SW_K]_t - C_K\left(x^0_{K,t}\right)\right\}. \tag{80}$$

C. PROOF OF PROPERTIES

The incentive compatibility properties of the above settlement schemes will be demonstrated in this section. Taking EPs as an example, when J-th EP declares the true cost c_J, and other EPs declare any cost $\hat{c}_{-J}$, the payment to EP J is given as

$$\mathbf{S}_J^{**} = f\left(X^{**}, c_J, \hat{c}_{-J}\right) + C_J\left(X_J^{**}\right) - f_{-J}\left(X_{-J}^{*}, \hat{c}_{-J}\right). \quad (81)$$

where $f(\cdot)$ is the social welfare. X^{**} is the optimal energy supply scheme when when J-th EP declares the true cost and other EPs declare any cost, namely

$$X^{**} \in \arg\min f\left(X, c_J, \hat{c}_{-J}\right). \quad (82)$$

The net income of J-th EP is given as

$$\begin{aligned}\delta^{**} &= \mathbf{S}_J^{**} - C_J\left(X_J^{**}\right) \\ &= f\left(X^{**}, c_J, \hat{c}_{-J}\right) + C_J\left(X_J^{**}\right) - f_{-J}\left(X_{-J}^{**}, \hat{c}_{-J}\right) \\ &\quad - C_J\left(X_J^{**}\right) \\ &= \mathbf{R}\left[SW_{-J}^{**}\right] - C_J\left(X_J^{**}\right) - f_{-J}\left(X_{-J}^{**}, \hat{c}_{-J}\right). \end{aligned} \quad (83)$$

When J-th EP declares the untrue cost $\hat{c}_J$, and other EPs declare any cost $\hat{c}_{-J}$, the payment to EP J is given as

$$\mathbf{S}_J^{*} = f\left(X^{*}, \hat{c}_J, \hat{c}_{-J}\right) + C_J\left(X_J^{*}\right) - f_{-J}\left(X_{-J}^{*}, \hat{c}_{-J}\right). \quad (84)$$

where X^* is the optimal energy supply scheme when when J-th EP declares the true cost and other EPs declare any cost, namely

$$X^{*} \in \arg\min f\left(X, \hat{c}_J, \hat{c}_{-J}\right). \quad (85)$$

Now the net income of J-th EP can be given as

$$\begin{aligned}\delta^{*} &= \mathbf{S}_J^{*} - C_J\left(X_J^{*}\right) \\ &= f\left(X^{*}, \hat{c}_J, \hat{c}_{-J}\right) + C_J\left(X_J^{*}\right) - f_{-J}\left(X_{-J}^{*}, \hat{c}_{-J}\right) \\ &\quad - C_J\left(X_J^{*}\right) \\ &= \mathbf{R}\left[SW_{-J}^{*}\right] - C_J\left(X_J^{*}\right) - f_{-J}\left(X_{-J}^{*}, \hat{c}_{-J}\right). \end{aligned} \quad (86)$$

Note that the first item on the right end of (83) and (86) is only related to the reported operation cost of other EPs. So the difference value between δ^{**} and δ^{*} is calculated by (87).

$$\begin{aligned}&\delta^{**} - \delta^{*} \\ &\quad = \mathbf{R}\left[SW_{-J}^{**}\right] - C_J\left(X_J^{**}\right) - \mathbf{R}\left[SW_{-J}^{*}\right] + C_J\left(X_J^{*}\right) \\ &\quad = \mathbf{R}\left[SW_J^{**}\right] - \mathbf{R}\left[SW_J^{*}\right] \end{aligned} \quad (87)$$

If the EPs make a strategic reports, that is, the reported value deviates from the true marginal cost, or the EPs exit the IEM, it will make it difficult for the market clearing plan to maximize social welfare. Therefore, (87) is non-negative. That is, the net profit of J-th EP obtained by reporting the truthful cost is not less than the net profit at the time of truthless submission of cost. Such a result indicates that the true marginal cost of each EP submission is its optimal choice, rather than the strategic reporting of truthless costs.

Similarly, the same proof method can be used for ELs.

D. BUDGET IMBALANCE REDISTRIBUTION UNDER THE VCG MECHANISM

Applying the truthful submission of the marginal cost of each EP as the dominant market strategy has been proven to guarantee that the payment received by each EP cannot be less than its marginal cost [9]. As such, the revenue received by an EP must necessarily be greater or equal to its operational cost if its profit is non-negative. However, the VCG mechanism cannot guarantee such a budget balance [26]. We define the budget imbalance in the IEM as follows:

$$S_{BI,t} = \sum_{K \in \Omega_{EL}} \mathbf{S}_{K,t} - \sum_{J \in \Omega_{EP}} \mathbf{S}_{J,t}. \quad (88)$$

A value $S_{BI,t} < 0$ indicates that the IEM has a budget deficit while $S_{BI,t} > 0$ indicates that the IEM has a budget excess, and the payments should be redistributed to the market participants accordingly. A fair and reasonable redistribution mechanism requires that the redistribution mechanism correspond to the individual contribution of each market participant to the revenue adequacy of the IEM [26]. Here, we solve the market clearing problem after excluding each market participant α in turn, and calculate the budget imbalance $S_{-\alpha,t}$ without α. Note that α can be either an EP or an EL. If $S_{-\alpha,t} > 0$ and $S_{BI,t} < 0$, then the participation of α in the market contributes toward a negative budget imbalance, and α should be charged accordingly. In contrast, when $S_{BI,t} > 0$, we can conclude that α contributes toward the budget excess if $S_{-\alpha,t} < S_{BI,t}$, and α should be rewarded accordingly. Finally, if α is found to have no effect on the budget imbalance, then the revenue of α is not affected by the redistribution mechanism. Accordingly, the proposed redistribution mechanism can distinguish those participants whose market participation jeopardizes revenue adequacy and those whose participation is contributing toward achieving revenue adequacy.

After determining the contribution of each participant to the budget imbalance, we must then determine the amount of funds that must be accordingly redistributed to each participant. We define the amount of the redistributed payment as

$$q_{RM,\alpha,t} = \frac{S_{-\alpha,t}}{N_\alpha}. \quad (89)$$

where N_α is the number of market participants. Under conditions where revenue adequacy is not satisfied (i.e., $S_{BI,t} < 0$), the cost recovery of each participant is imposed under an ex-post redistribution mechanism based on the total profit of the participant and the amount determined by (71). More specifically, if the total profit of the participant is positive, then the redistribution payment calculated by (71) is applied directly as the compensation. However, if the total profit of the participant is negative, then the redistribution payment calculated by (89) is increased so that it exactly compensates for the negative profit of the participant, which results in a zero total profit for the participant. Similarly, under conditions where revenue adequacy is satisfied (i.e., $S_{BI,t} > 0$),

each participant that contributes toward a positive budget imbalance is rewarded by an amount $q_{RM,\alpha,t}$.

The advantages of the above redistribution mechanism have been described and analyzed elsewhere [9]. This mechanism does not affect the efficiency of the two-stage IEM, and ensures ex-post cost recovery by constraining the redistribution payment according to the VCG profit/utility of each participant.

V. ILLUSTRATIVE EXAMPLES

A. BASIC CONFIGURATIONS

The validity of the proposed model and method were verified by application to the RIES illustrated in Fig. 2, which is composed of a 33-bus DES, an 11-node DGS [26], and the 33-node DHS of the Barry Island heat network installation [27]. The reported marginal costs of the EPs are listed in Table 1.

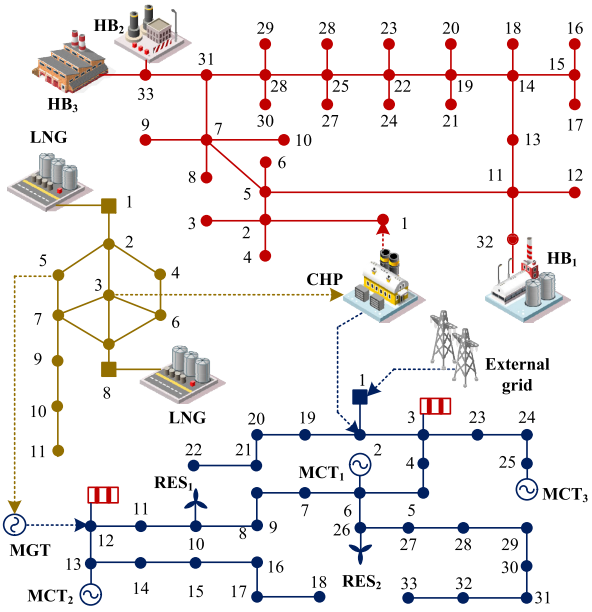

FIGURE 2. Schematic illustrating the test case RIES.

TABLE 1. Declared marginal costs of the EPs illustrated in Fig. 2.

EP	Marginal cost ($/kW$)	EP ($)	Marginal cost ($/kW$)
MCT_1	0.64	HB_3	1.52
MCT_2	0.60	LNG_1	1.20
MCT_3	0.60	LNG_2	1.02
HB_1	0.60	EG_2	1.20
HB_3	1.50		

B. SCENARIO DATA

The base case energy requirements for the test RIES over a 24 h period are shown in Fig. 3 based on real-world data obtained from the PJM market of America. The total electric load is 3.71 MW, the total gas load is 1.98 MW, and the total heat load is 1.90 MW over the 24 h period. The RES output scenario data is shown in Fig. 4 based on real-world

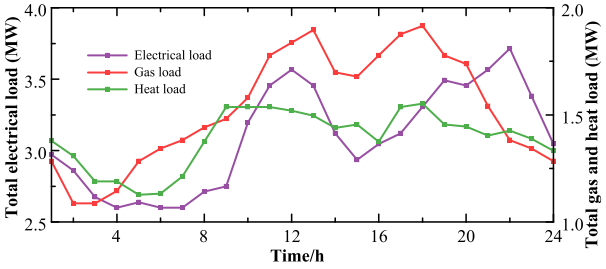

FIGURE 3. Energy requirements for the test case RIES.

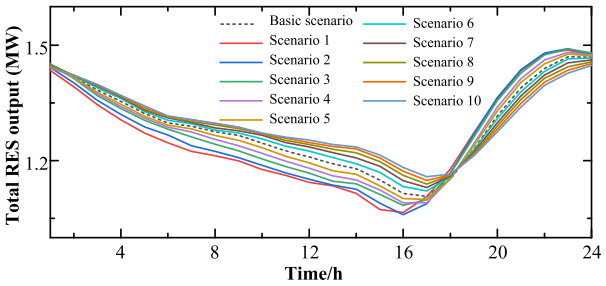

FIGURE 4. RES output scenario data for the test case RIES.

historical RES output data obtained from the National Energy Laboratory over a 24 h period with a total installed capacity of 1.7 WM. Ten stochastic scenarios and the basic scenario were obtained by applying scenario reduction techniques to the historical data.

C. CASE STUDY 1

The convertibility and complementarity of energy sources in the RIES is a major advantage affecting the efficiency of integrated systems. However, unsynchronized changes in electricity, gas, and heat demands can affect the clearing and settlement of the IEM. Hence, we designed the following cases to research the effect of energy demand increases on the incentive compatibility mechanism.

1) Case 1A: base-case demands.
2) Case 1B: heat demand increased by 20%.
3) Case 1C: heat demand increased by 40%.

TABLE 2. Demand utility, system cost, and social welfare of the different cases.

Case	Total demand utility (10^7 \$)	Total system cos (10^5 \$)	Total social welfare (10^7 \$)
Case 1A	1.442	2.473	1.418
Case 1B	1.509	82.591	1.483
Case 1C	1.570	2.700	1.543

1) IMPACTS OF HEAT DEMAND ON DEMAND UTILITY, SYSTEM COST, AND SOCIAL WELFARE

Table 2 shows the total demand utility, system cost, and social welfare for the three different cases over the 24 h period, where the social welfare is the difference between the

demand utility and the system cost. The total demand utility of Case 1B and Case 1C respectively increased by 4.64% and 8.87% compared with Case 1A, the total system cost increased by 4.77% and 9.18%, respectively, and the total social welfare increased by 4.58% and 8.82%, respectively. It can be seen from the above results that, although the increases in heat demand increased the operating cost of the system, these also increased the total social welfare to some extent.

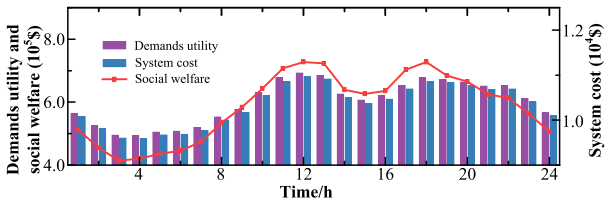

FIGURE 5. Periodic demand utility, system cost, and social welfare of Case 1A.

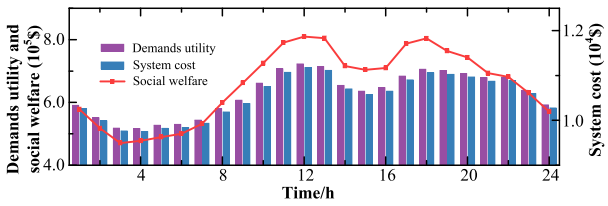

FIGURE 6. Periodic demand utility, system cost, and social welfare of Case 1B.

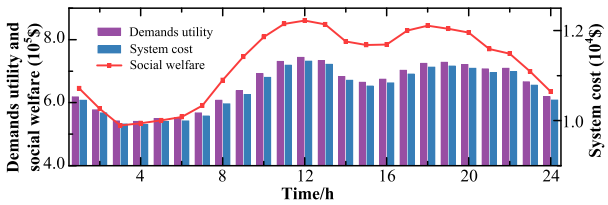

FIGURE 7. Periodic demand utility, system cost, and social welfare of Case 1C.

Figures 5, 6, and 7 present the demand utility, system cost, and social welfare obtained at each time period over the complete 24 h scheduling period for Cases 1A, 1B, and 1C, respectively. It can be seen that the social welfare over the period of high energy demand from 10:00 to 22:00 is greater than that over the low-load periods, and that the social welfare in any period increases with increasing heat load. This is because, on the one hand, an increase in heating demand promotes the consumption of RES output, while, on the other hand, the access ratio of demand in the real-time market increases, and the total utility of energy demands increases, which will eventually increase the total social welfare of the RIES.

2) IMPACTS OF HEAT DEMAND ON EP REVENUES

The high degree of coupling between energy sources in the RIES causes changes in one subsystem to affect the other

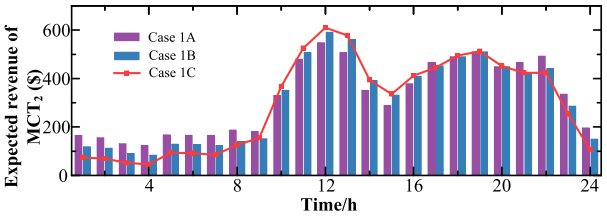

FIGURE 8. Revenue of MCT_2 under different test cases.

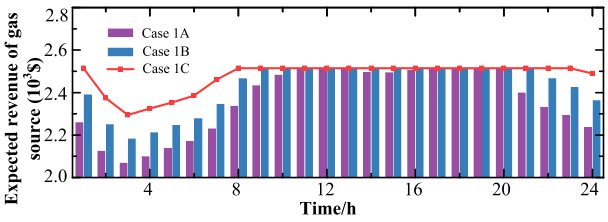

FIGURE 9. Revenue of the LNG source at node 8 under different test cases.

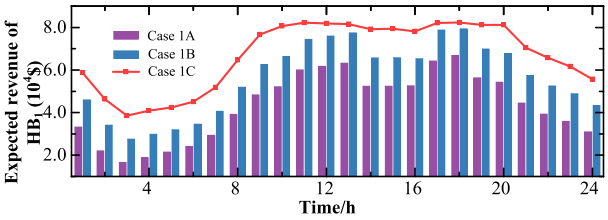

FIGURE 10. Revenue of HB_1 under different test cases.

subsystems through the coupling devices, which then affects the revenues of EPs. Therefore, we plot the periodic expected revenues of representative EPs in the test RIES under the three test cases in Figs. 8 to 10.

It can be seen from Fig. 8 that the revenue of MCT_2 decreases with increasing heat demand during the periods of 01:00-08:00 and 21:00-24:00. At all other times, the revenues under Case 1B and Case 1C are greater than those under Case 1A. In addition, the heat generation of the CHP increases as the heat load increases because the CHP is operated in the ''power determined by heat'' mode, which also results in an increase in the CHP supply of electrical energy to the DES. However, the electric load during the periods of 01:00-08:00 and 21:00-24:00 (Fig. 3) is relatively low and the RES output (Fig. 4) is relatively high. These conditions reduce the active output of MCT_2, which ultimately leads to a decrease in revenue.

We note from Fig. 9 that the revenue of the LNG source at node 8 increases during the periods of 01:00-08:00 and 21:00-24:00 with increasing heat load. According to the VCG mechanism, the highest benefit can only be obtained when the EP declares its true marginal price. Therefore, the constant revenue observed for this LNG source between 09:00 and 20:00 may occur despite the increasing heat load because the declaration of marginal cost for this EP is truthful during

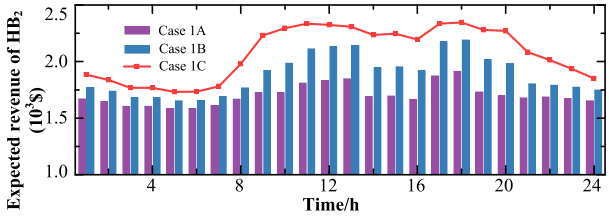

FIGURE 11. Revenue of HB_2 under different test cases.

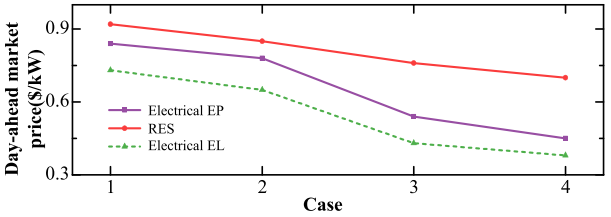

FIGURE 12. Day-ahead market prices of participants in the DES.

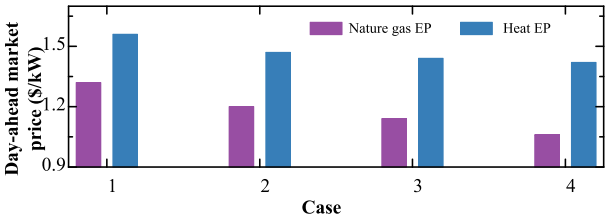

FIGURE 13. Day-ahead market prices of participants in the DGS and DHS.

this period. In other words, the maximum profit has been obtained for this EP.

The revenues of HB_1 and HB_2 are respectively shown in Figs. 10 and 11. It can be seen that the revenues of the two EPs are very different. On the one hand, HB1 is highly competitive in the IEM because it has a low energy unit production cost, and therefore contributes more to the RIES than the other HBs. On the other hand, the truthful declared marginal costs of thermal energy production helps the EP to increase profits, particularly during high load periods. We also note that the revenues of the HBs decreased relatively little between 13:00 and 16:00 for Case 1C, compared to the corresponding reductions for Case 1A and Case 1B. This is because the increased heat load ensures that the actual marginal cost is close to the declared marginal cost of the CB to some extent, and the HB has attained the maximum benefit of the IEM.

D. CASE STUDY 2

The RES penetration level and the uncertainty of RES output have a significant impact on the settlement of each member of the IEM. Therefore, we designed the following cases to investigate the impact of RES penetration and output uncertainty on market imbalances under the proposed IEM methodology.

1) Case 2A: base-case RES generation.
2) Case 2B: installed RES capacity increased by 20%.
3) Case 2C: installed RES capacity increased by 40%.
4) Case 2D: installed RES capacity increased by 60%.

These cases are applied under the assumption that the RES output always represents the same proportion of the installed capacity. Moreover, the total energy demand of the ELs is reduced by 15%. We note that the steadily increasing RES capacity in the four test cases represents steadily increasing penetration levels and RES output uncertainties.

TABLE 3. Demand utility, system cost, and social welfare of the different test cases.

Case	Total demand utility (10^7 \$)	Total system cos (10^5 \$)	Total social welfare (10^7 \$)
Case 2A	1.342	2.143	1.321
Case 2B	1.437	2.097	1.416
Case 2C	1.494	2.057	1.473
Case 2D	1.528	2.006	1.508

It can be seen from Table 3 that the total cost of the RIES decreases with increasing RES capacity, while the total demand utility and total social welfare increase with a gradually reducing growth rate. This is due to the limited ability of the RIES to absorb the increasing RES output, and the RES output that cannot be absorbed by the RIES or sold on the IEM can only be abandoned, which is not conducive to the efficient use of energy, and also represents a loss of social welfare.

1) IMPACT OF RES OUTPUT ON THE DAY-AHEAD MARKET PRICE

We define the weighted average price at which an EP is paid as the sum of all individual prices multiplied by the ratio of the individual price to the total traded power in day-ahead market:

$$\hat{\lambda}_{EP,t} = \sum_{J\in\Omega_{EP}} \frac{\mathbf{S}_{J,t}}{\sum\limits_{J\in\Omega_{EP}} p^0_{J,t}}. \tag{90}$$

Similarly, the weighted average price at which an EL is charged can be defined as

$$\hat{\lambda}_{EL,t} = \sum_{K\in\Omega_{EL}} \frac{\mathbf{S}_{K,t}}{\sum\limits_{K\in\Omega_{EL}} p^0_{K,t}}. \tag{91}$$

As can be seen from Fig. 12, the day-ahead market price paid by electrical ELs decreases as the RES capacity increases. Simultaneously, we note that the lower marginal cost of stochastic EPs than that of conventional EPs increase their competitiveness in the IEM. Therefore, the increasing RES capacity has a greater impact on the day-ahead market price paid to conventional EPs than stochastic EPs. However, the tight coupling between energy sources in the RIES ensure that the impact of RES output on the DES will also be propagated to the other two subsystems. Accordingly, we note from Fig. 13 that the day-ahead market prices of the heat EPs and natural gas EPs also decrease with increasing RES capacity.

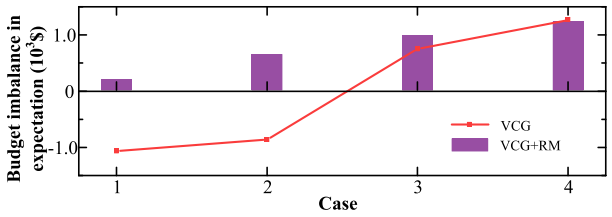

FIGURE 14. Budget imbalance in expectation before and after applying the proposed budget imbalance redistribution.

2) IMPACT OF RES CAPACITY ON BUDGET IMBALANCE

From Fig. 14, we can see that the VCG mechanism leads to income and expenditure imbalances in the two-stage IEM, but that an increasing RES capacity helps to alleviate the problem. For relatively low RES capacities (Case 2A and Case 2B), the market budget is expected to be unbalanced because the total amount charged to the ELs by the IEMO is less than the total amount paid to the EPs. However, this situation changes when the RES capacity is increased. We also note from a comparison of the two plots in Fig. 14 that the application of the income redistribution mechanism can solve the imbalance between IEM revenue and expenditure. Here, we observe that the negative budget imbalances formerly obtained under relatively low RES capacities are fully restored and become positive after redistribution. In addition, rewarding market members who contribute toward revenue adequacy can reduce budget imbalances when income is adequately redistributed.

VI. CONCLUSION

This paper proposed a two-stage market clearing and settlement mechanism based on the VCG auction to achieve maximum market efficiency by properly motivating IEM participants to truthfully declare their marginal costs via the adoption of compatible market incentives. The VCG mechanism ensures cost recovery for all market participants by assigning energy prices according to the impact of participants on social welfare. The effects of load fluctuations and varying RES capacities on the market clearing and settlement mechanism were analyzed by conducting simulations for a realistic RIES. The results of this extensive analysis help foster a greater understanding of the functioning of the VCG mechanism and incentive compatibility in energy markets. In addition, we applied an after-the-fact solution to compensate for potential negative budget imbalances caused by the VCG auction mechanism.

REFERENCES

[1] Y. Zhou, Z. Wei, G. Sun, K. W. Cheung, H. Zang, and S. Chen, "A robust optimization approach for integrated community energy system in energy and ancillary service markets," *Energy*, vol. 148, pp. 1–15, Apr. 2018.

[2] J. M. Morale, A. J. Conejo, and K. Liu, "Pricing electricity in pools with wind producers," *IEEE Trans. Power Syst.*, vol. 27, no. 3, pp. 1366–1376, Aug. 2012.

[3] J. Zhang, B. Ge, and H. Xu, "An equivalent marginal cost-pricing model for the district heating market," *Energy Policy*, vol. 63, pp. 1224–1232, Dec. 2013.

[4] E. de Villemeur and P. O. Pineau, "Integrating thermal and hydro electricity markets: Economic and environmental costs of not harmonizing pricing rules," *Energy J.*, vol. 37, no. 1, pp. 77–100, Jan. 2016.

[5] J. Wang, Z. Wei, B. Yang, Y. Yong, M. Xue, G. Sun, H. Zang, and S. Chen, "Two-stage integrated electricity and heat market clearing with energy stations," *IEEE Access*, vol. 7, pp. 44928–44938, 2019.

[6] J. Wang, H. Zhong, Z. Ma, Q. Xia, and C. Kang, "Review and prospect of integrated demand response in the multi-energy system," (in English), *Appl. Energy*, vol. 202, pp. 772–782, Sep. 2017.

[7] F. A. Wolak, "Measuring unilateral market power in wholesale electricity markets: The California market, 1998–2000," *Amer. Econ. Rev.*, vol. 93, no. 2, pp. 425–430, May 2003.

[8] V. Moutinho, A. C. Moreira, and J. Mota, "Do regulatory mechanisms promote competition and mitigate market power? Evidence from Spanish electricity market," *Energy Policy*, vol. 68, pp. 403–412, May 2014.

[9] L. Exizidi, J. Kazempour, and A. Papakonstantinou, "Incentive-compatibility in a two-stage stochastic electricity market with high wind power penetration," *IEEE Trans. Power Syst.*, vol. 34, no. 4, pp. 2846–2858, Jul. 2019.

[10] C. M. Marrone, J. L. Bass, and C. J. Klinger, "Survey of medical liaison practices across the pharmaceutical industry," *Drug Inf. J.*, vol. 41, no. 4, pp. 457–470, Jul. 2007.

[11] Y. Xu and S. H. Low, "An efficient and incentive compatible mechanism for wholesale electricity markets," *IEEE Trans. Smart Grid*, vol. 8, no. 1, pp. 128–138, Jan. 2017.

[12] W. Tang and R. Jain, "Aggregating correlated wind power with full surplus extraction," *IEEE Trans. Smart Grid*, vol. 9, no. 6, pp. 6030–6038, Nov. 2018.

[13] J. E. Contreras-Ocana, M. A. Ortega-Vazquez, and B. Zhang, "Participation of an energy storage aggregator in electricity markets," *IEEE Trans. Smart Grid*, vol. 10, no. 2, pp. 1171–1183, Mar. 2019.

[14] T. Kwon, "Rent and rent-seeking in renewable energy support policies: Feed-in tariff vs. Renewable portfolio standard," *Renew. Sustain. Energy Rev.*, vol. 44, pp. 676–681, Apr. 2015.

[15] S. Chen, Z. Wei, G. Sun, K. W. Cheung, D. Wang, and H. Zang, "Adaptive robust day-ahead dispatch for urban energy systems," *IEEE Trans. Ind. Electron.*, vol. 66, no. 2, pp. 1379–1390, Feb. 2019.

[16] Z. Zhou, J. Zhang, P. Liu, Z. Li, M. C. Georgiadis, and E. N. Pistikopoulos, "A two-stage stochastic programming model for the optimal design of distributed energy systems," *Appl. Energy*, vol. 103, pp. 135–144, Mar. 2013.

[17] Z. Luo, Z. Wu, Z. Li, H. Cai, B. Li, and W. Gu, "A two-stage optimization and control for CCHP microgrid energy management," *Appl. Therm. Eng.*, vol. 125, pp. 513–522, Oct. 2017.

[18] G. Mavromatidis, K. Orehounig, and J. Carmeliet, "Comparison of alternative decision-making criteria in a two-stage stochastic program for the design of distributed energy systems under uncertainty," *Energy*, vol. 156, pp. 709–724, Aug. 2018.

[19] A. Ahmadi, M. Charwand, and P. Siano, "A novel two-stage stochastic programming model for uncertainty characterization in short-term optimal strategy for a distribution company," *Energy*, vol. 117, pp. 1–9, Dec. 2016.

[20] B. F. Hobbs, M. H. Rothkopf, and L. C. Hyde, "Evaluation of a truthful revelation auction in the context of energy markets with nonconcave benefits," *J. Regulatory Econ.*, vol. 18, no. 1, pp. 5–32, Jun. 2000.

[21] R. Li, W. Wei, and S. Mei, "Participation of an energy hub in electricity and heat distribution markets: An MPEC approach," *IEEE Trans. Smart Grid*, vol. 10, no. 4, pp. 3641–3653, Jul. 2018.

[22] Z. Zhao and L. Wu, "Impacts of high penetration wind generation and demand response on LMPs in day-ahead market," *IEEE Trans. Smart Grid*, vol. 5, no. 1, pp. 220–229, Jan. 2014.

[23] S. Chen, Z. Wei, G. Sun, K. W. Cheung, and Y. Sun, "Multi-linear probabilistic energy flow analysis of integrated electrical and natural-gas systems," *IEEE Trans. Power Syst.*, vol. 32, no. 3, pp. 1970–1979, May 2017.

[24] S. Pan and J.-S. Chen, "Interior proximal methods and central paths for convex second-order cone programming," *Nonlinear Anal.*, vol. 73, no. 9, pp. 3083–3100, Nov. 2010.

[25] Z. Wei, J. Sun and Z. Ma, "Chance-constrained coordinated optimization for urban electricity and heat networks," *CSEE J. Power Energy Syst.*, vol. 4, no. 4, pp. 399–407, Dec. 2018.

[26] R. B. Myerson and M. A. Satterthwaite, "Efficient mechanisms for bilateral trading," *J. Econ. Theory*, vol. 29, no. 2, pp. 265–281, Apr. 1983.

[27] M. Abeysekera, J. Wu, and N. Jenkins, "Steady state analysis of gas networks with distributed injection of alternative gas," *Appl. Energy*, vol. 164, pp. 991–1002, Feb. 2016.
[28] X. Liu, J. Wu, N. Jenkins, and A. Bagdanavicius, "Combined analysis of electricity and heat networks," *Appl. Energy*, vol. 162, pp. 1238–1250, Jan. 2016.

MANYUN HUANG received the B.S. degree from the College of Energy and Electrical Engineering, Hohai University, Nanjing, China, in 2014, and the joint Ph.D. degree from RWTH Aachen University, Germany, in 2018. She is currently pursuing the Ph.D. degree with Hohai University.

Her research interests include the theory and algorithms of power system state estimation and Kalman filter.

ZHINONG WEI received the B.S. degree from the Hefei University of Technology, Hefei, China, in 1984, the M.S. degree from Southeast University, Nanjing, China, in 1987, and the Ph.D. degree from Hohai University, Nanjing, in 2004.

He is currently a Professor of electrical engineering with the College of Energy and Electrical Engineering, Hohai University. His research interests include power system state estimation, integrated energy systems, smart distribution systems, optimization and planning, load forecasting, and the integration of distributed generation into electric power systems.

PING JU received the B.S. and M.S. degrees from Southeast University, Nanjing, China, in 1982 and 1985, respectively, and the Ph.D. degree from Zhejiang University, Hangzhou, China, all in electrical engineering. He is currently a Professor of electrical engineering with Hohai University, Nanjing, China, and also with Zhejiang University, Hangzhou, China. From 1994 to 1995, he was an Alexandervon Humboldt Fellow with the University of Dortmund, Germany.

His research interests include modeling and control of power system with the integration of renewable generation.

JINRAN WANG received the B.S. degree from the Information Engineering College of Nanchang University, Nanchang, China, in 2017. He is currently pursuing the M.S. degree in electrical engineering with Hohai University.

His research interests include the theory and algorithms of regional integrated energy systems.

SHENG CHEN received the B.S. and Ph.D. degrees from the College of Energy and Electrical Engineering, Hohai University, Nanjing, China, in 2014 and 2019, respectively. From January 2018 to January 2019, he was a Visiting Scholar with The Ohio State University, Columbus, OH, USA.

He is currently an Associate Professor with the College of Energy and Electrical Engineering, Hohai University. His research interests include integrated energy systems, operations research, and electricity markets.